ISSN: 2319-8753

International Journal of Innovative Research in Science, Engineering and Technology

(An ISO 3297: 2007 Certified Organization)

Vol. 3, Issue 8, August 2014

A Novel Technique for Synthesis A Thermal Barrier Coating Material of Lanthanum – Magnesium Hexaaluminate ($LaMgAl_{II}O_{19}$)

Q. Mohsen [1]

[1] Materials & Corrosion Group, Taif University, Saudi Arabia

ABSTRACT: As the advances in some industrial applications are leading to higher operating temperatures; materials of metallic coatings that withstand harsh environments at high temperature are developing. One of the most promising compounds, which can be used as a material for thermal barrier coatings (TBCs) is lanthanum magnesium hexaaluminate ($LaMgAl_{11}O_{19}$).The objective of this study, was to synthesize $LaMgAl_{II}O_{19}$ through a technique of tartaric acid precursor. Effect of different annealing temperature on the microstructure has been studied and reported in the presented research. The annealing temperature was controlled from 900-1300 ^oC. Kinetic calculations confirmed by the experimental data from the thermal analyses were used to assess the nature of the resultant compound. Interpretation of FT-IR and XRD spectra combined with SEM-EDX observations have identified that a pure single phase was successfully obtained at 1100 ^oC.

KEYWORDS: Thermal barrier coatings; lanthanum magnesium hexaaluminate; annealing temperature; tartaric acid.

I. INTRODUCTION

Over the past decades, advances in coating technology have resulted in its possible commercial exploitation in providing the necessary protection for materials in high temperature applications. One the most promising high-temperature materials are hexaaluminates. They are compounds with the general structure of $A^{2+}B_{12}{}^{3+}$ O_{19} [1], and they contain alkali, alkaline earth or rare earth metal, with Beta – Al_2O_3 or magnetoplumbite – type crystal structure [2].This class of hexaaluminates, has been utilized as a material for thermal barrier coatings (TBCs) [3]. Typically, thermal barrier coatings are composed of two important layers; the first one is a porous, insulating ceramic oxide top layer of yttria-stabilized with zirconia (YSZ), which provides thermal protection. The second layer is a metallic bond coat, which provides oxidation and hot corrosion protection [4, 5]. For integration into the TBCs, materials require low thermal conductivity, sufficiently high thermal expansion coefficient, phase stability up to temperatures higher than 1400^oC, stable pore morphology, chemical and mechanical compatibility with the underlying layers [6]. It is therefore, of great importance to compensate the loss in mechanical properties of zirconia-containing materials through the incorporation of other dispersoids [7]. This can maintain good toughness and strength. The increase in thermal conductivity of coatings caused by densification, due to increasing the operating temperature is an additional important issue, which reveals the need for materials with low sinterability at elevated temperatures. These materials should substitute YSZ for long-term high temperature applications due to common problems with YSZ (e.g., dramatic aging at temperatures above 1100 ^oC and post sintering, which reduces the thermal conductivity). Since, oxygen diffusivity of zirconia increases with temperature and leads to constant oxidation of the bond layer and consequently failure of the TBCs in operation. Materials with lower oxygen diffusivity are required as well [8]. Lanthanum magnesium hexaaluminate ($LaMgA_{II}1O_{19}$), with a magnetoplumbite crystal structure and a plate-like grain structure have the potential to be applied as material of TBCs. Although, the thermal conductivity of ($LaMgA_{II}1O_{19}$)(0.8–2.6Wm^{-1} K^{-1}) is to some extent higher than that of YSZ (0.6–2.3Wm^{-1} K^{-1}), however its low Young's modulus, low sinterability, superior structural, thermochemical stability up to 1400^oC, stable pore structure, and lower oxygen diffusivity, draw attentions to investigate ($LaMgA_{II}1O_{19}$) as a candidate material for TBCs [9-12].The aim of this study is to use tartaric acid gel method, in order to achieve fully crystallized $LaMgAl_{11}O_{19}$ oxide at relatively low temperature.

DOI: 10.15680/IJIRSET.2014.0308081

ISSN: 2319-8753

International Journal of Innovative Research in Science, Engineering and Technology

(An ISO 3297: 2007 Certified Organization)

Vol. 3, Issue 8, August 2014

II. EXPERIMENTAL

Tartrate precursor method was applied for the synthesis of $LaMgA_{ll}1O_{19}$. Tartaric acid precursor technique involves the preparation of aqueous solution of the required cation, the chelation of cations in solution by addition of tartaric acid then; raising the temperature of the solution until the precursor is formed. Pure chemical grade of, aluminum nitrate ($Al(NO_3)_3$, lanthanum nitrate ($La(NO_3)_3$, magnesium chloride ($MgCl_2$), in the presence of stoichiometric amount of tartaric acid were used as starting materials. The mixtures of La-Mg-Al solution, firstly prepared and then stirred for 15 minute on hot plate magnetic stirrer, followed with addition of an aqueous solution of tartaric acid to the mixtures with stirring. Then, the solution was evaporated to 80°C with constant stirring until dryness, and left overnight to dry again at 100°C. The dried powders obtained as aluminate precursor. Lanthanum hexaaluminate ($LaMgAl_{ll}O_{19}$) powders synthesized by the sol–gel and calcination method at 1100 °C for 2h exhibit a single hexaaluminate phase. The sol–gel and calcination method have a particle size of 5–30μm, and exhibit to a certain extent agglomeration. Differential thermal analysis of the un-annealed precursor was carried out with heating rate at 10°C/min; between room temperature and 1200°C. The measurements were performed in a current of nitrogen atmosphere. Phase composition and structure was determined using X-ray diffraction (XRD) analysis. The analyses were performed on a Brucker axis D8 diffractometer using Cu-K_α (λ= 1.5406) radiation and secondary monochromator in the range 2θ from 10^0 to 70^0. Then, identity of the present phases was determined by matching the experimental pattern with standards compiled by the Joint Committee on Powder Diffraction Standards (JCPDS). Spectra of FT-IR of lanthanum magnesium hexaaluminate, $LaMgAl_{ll}O_{19}$,at different temperatures (1100, 1200 and 1300 °C) were recorded on a Bruker FT-IR spectrometer equipped without using potassium bromide discs and with a resolution of 4 cm^{-1} 40 scans .The morphology of the synthesized particles was directly imaged and determined using scanning electron microscopy (SEM,JSM-5400). Qualitative analysis for the different elements in the powders was used to clarify the distribution of each element of La, Mg, Al and O. by Energy Dispersive X-ray spectroscopy (EDX).

III. RESULTS AND DISCUSSIONS

3.1. Infrared spectra

Heating the parent sample (Formula 1) at temperatures ranging from 300 to 580 °C for 1hr. (Fig.1) leads to appearance of growing bands in the carbonate/carboxylate region. The broad band at 1410 cm^{-1} is attributed to the ν3 vibration of mono-dentate carbonates [13, 14]. Weak absorptions at 2900, 2800 and 2600 cm^{-1} together with the band at 1500 cm^{-1} are typical of tartrate species [13, 14]. The former three bands are due to Fermi resonance between the ν(CH) fundamental and combinations or overtones of bands in the carboxylate region. The ν_{as}(COO) stretching vibration of the tartrate species is positioned at 1500 cm^{-1}, whereas the δ(CH) frequency coincides with the low frequency component of the ν_3 vibration at 1410 cm^{-1} of the monodentate carbonates. The intensities of the carbonate-carboxylate bands increase significantly at 300-580 °C temperature (Fig. 1). The spectra taken under these conditions contain broad absorption in the 3700–2900 cm^{-1} region corresponding to crystalline water molecules. FT-IR spectra Fig. 2 of lanthanum magnesiumhexaaluminate, $LaMgAl_{11}O_{19}$, were recorded at different temperatures of (1100, 1200 and 1300 °C). For the *in situ* FT-IR measurements; a sample of the lanthanum magnesium hexaaluminate calcined at 1100 °C, in the range of 1600–4000 cm^{-1}. The spectrum as shown in (Fig. 2) has no absorption peaks detected concerning of CO_2 and H_2O. By comparing the standard spectra of La_2O_3, MgO and Al_2O_3, the absorption peaks of $LaMgAl_{11}O_{19}$ powder are indexed as shown in Fig. 2. Those peaks are detected at (743 and 689) cm^{-1}, (657 and 518) cm^{-1}, and (457 and 419) cm^{-1} for the MgO, La_2O_3 and Al_2O_3, respectively. However, the absorption peaks of the $LaMgAl_{11}O_{19}$ before thermal treatment are weak and broadened, showing a character of non-perfect crystallization which is consistent with the XRD result. After thermal treatment, the re-crystallization was finished and its spectrum is very similar to that of the powder $LaMgAl_{11}O_{19}$.

ISSN: 2319-8753

International Journal of Innovative Research in Science, Engineering and Technology

(An ISO 3297: 2007 Certified Organization)

Vol. 3, Issue 8, August 2014

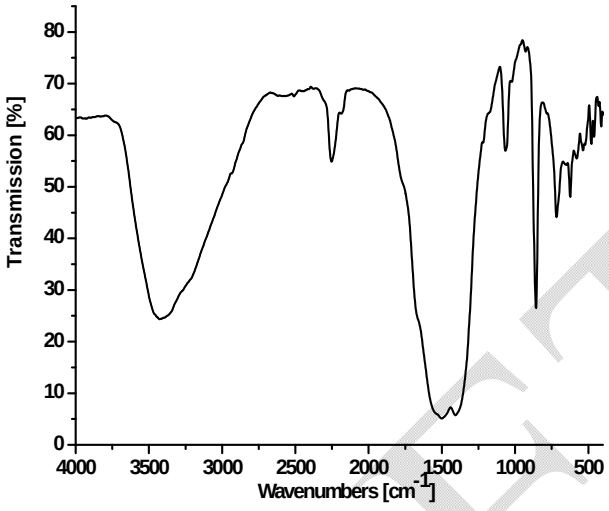

Fig. 1: FT-IR spectrum of solid La/Mg/Al-tartrate parent sample

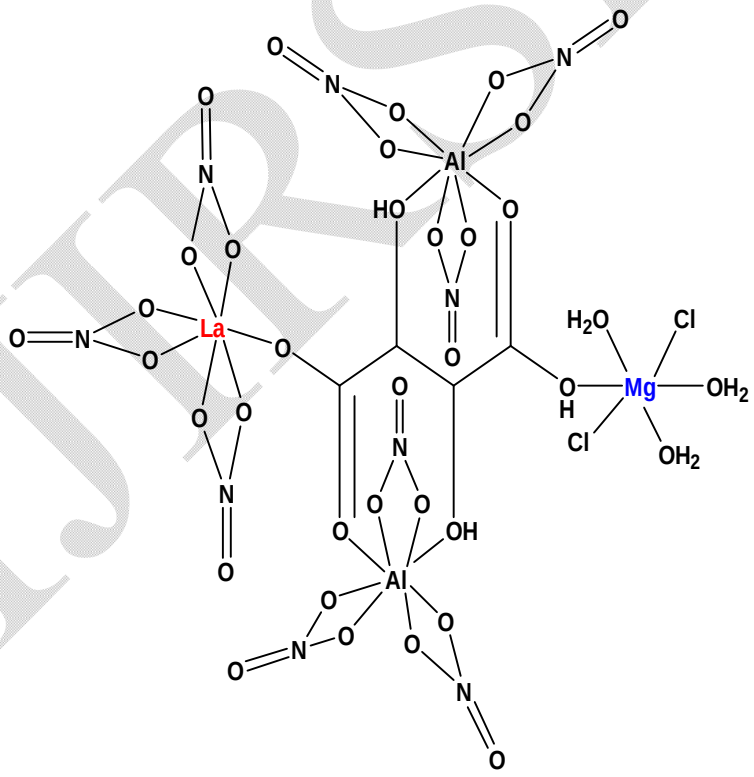

Formula I: Suggested structure of solid La/Mg/Al-tartrate parent sample.

ISSN: 2319-8753

International Journal of Innovative Research in Science, Engineering and Technology

(An ISO 3297: 2007 Certified Organization)

Vol. 3, Issue 8, August 2014

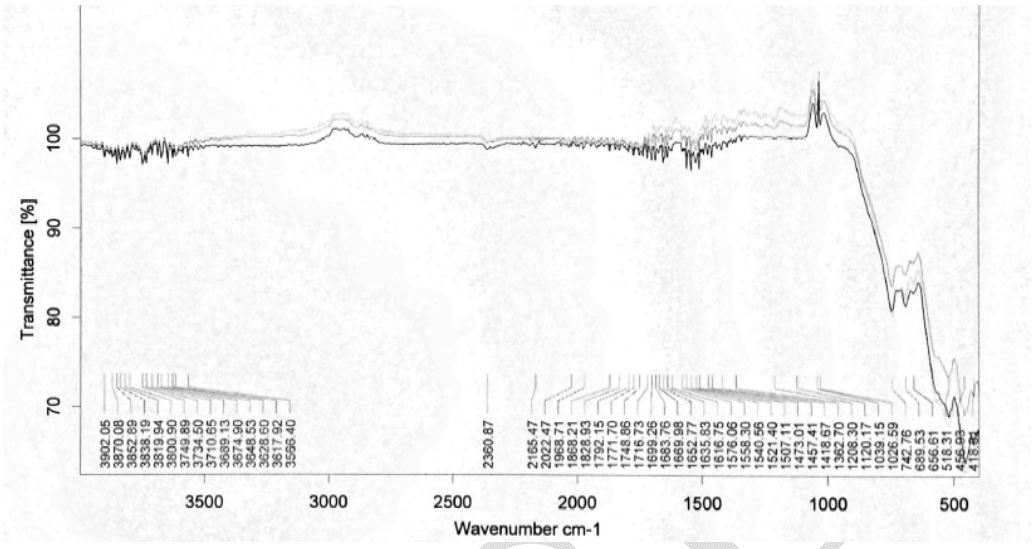

Fig. 2: FT-IR spectrum of solid lanthanum magnesiumhexaaluminate sample at different temperatures (1100, 1200 and 1300 ^{o}C)

3.2. Thermal analysis

In order to understand thermal decomposition of the formation of $LaMgAl_{11}O_{19}$compound; thermal gravimetric-differential thermal analyses with differential scanning calorimetric (TG-DTA-DSC) were carried out with a small amount of [$La(NO_3)_3.MgCl_2.11Al(NO_3)_3.nC_4H_6O_6$] parent sample and the result is shown in Fig. 3. The sample has three decomposition steps of weight loss starting at 180, 300 and 400 ^{o}C, respectively, leading to a total weight loss of approximately 40%. The first loss could be attributed to the loss of the adsorbed moisture. The most possible reason for other two steps is the loss of CO_2 and organic gases (methane/ethane or acetylene) species at preliminary temperatures. In air atmosphere and at high temperature, the oxide ceramic reacts with H_2 (tartaric organic specie) and the formation of hydroxide species is possible. The decomposition temperatures of hydroxide species in $La(OH)_3$, $Mg(OH)_2$ and $Al(OH)_3$ are 350–580 ^{o}C(15), 350 ^{o}C(16), and 300–420 ^{o}C [15, 16], respectively. The decomposition of carbonate species occurs at some higher temperature, for example, 670–810 ^{o}C for $La_2(CO_3)_3$(15), and 350–900 ^{o}C for $Mg(OH)_2.MgCO_3$(15). Herein this paper, the thermal decomposition technique of carbonate usually is assumed to intermediate stage in between two major steps parent adduct [$La(NO_3)_3.MgCl_2.11Al(NO_3)_3.nC_4H_6O_6$] (Formula I) and lanthanum magnesium hexaaluminate, $LaMgAl_{11}O_{19}$. Figure 3 illustrates a weight loss of the parent sample during the process. As the temperature increased between 200 to 600 ^{o}C (DSC = 400 ^{o}C) rapid dropped in the weight loss; according to formation of carbonate compound, $La_2(CO_3)_3.Mg(OH)_2.MgCO_3.11Al_2(CO_3)_3$, which escaped as a volatile gases like carbon mono and dioxide. Moreover, the sample weight seemed to be constant after the temperature reached 580 ^{o}C (a calcinations point). It signifies that the process was already done and the target compound of $LaMgAl_{11}O_{19}$ was formed successfully with 60% and a totally weight loss of 40%. The assumption for the preparation of lanthanum magnesium hexaaluminate was supported by the analysis that has been

done using XRD and will be described later. Steps of the thermal decomposition of the parent compound can be summarized in the following equations;

1- $2[La(NO_3)_3.MgCl_2.11Al(NO_3)_3.19C_4H_6O_6] \rightarrow La_2(CO_3)_3.Mg(OH)_2.MgCO_3.11Al_2(CO_3)_3+39CO_2+4HCl+72NO_2+54H_2O+27½O_2$

2- $La_2(CO_3)_3.Mg(OH)_2.MgCO_3.11Al_2(CO_3)_3 \rightarrow 2LaMgAl_{11}O_{19} + H_2O + 37CO_2$

DOI: 10.15680/IJIRSET.2014.0308081

ISSN: 2319-8753

International Journal of Innovative Research in Science, Engineering and Technology

(An ISO 3297: 2007 Certified Organization)

Vol. 3, Issue 8, August 2014

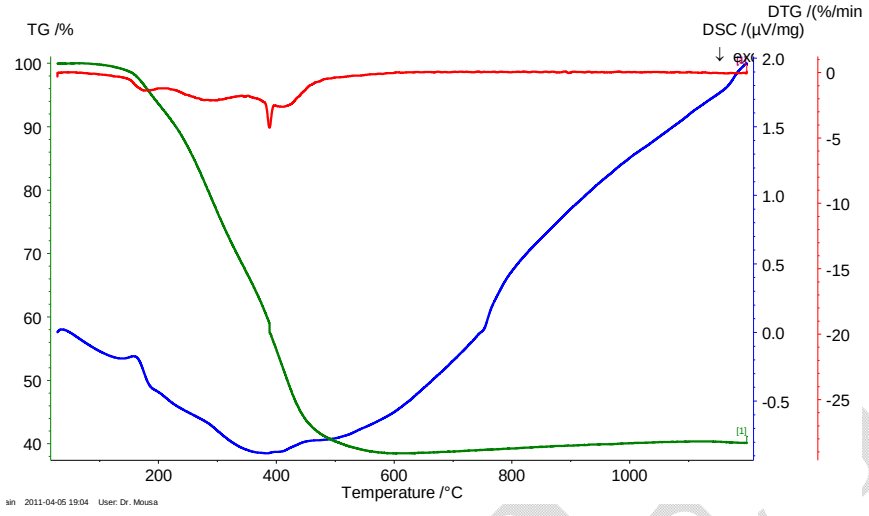

Fig.3: TG, DTG and DSC curve of $[La(NO_3)_3.MgCl_2.11Al(NO_3)_3.19C_4H_6O_6]$adduct.

3.3. Kinetic studies

In recent years there has been increasing interest in determining the rate-dependent parameters of solid-state non-isothermal decomposition reactions by analysis of TG curves. Several equations [17-22] have been proposed as means of analyzing a TG curve and obtaining values for kinetic parameters. Many authors [17-21] have discussed the advantages of this method over the conventional isothermal method. The rate of a decomposition process can be described as the product of two separate functions of temperature and conversion [18], using

$$d\alpha/dt = k(T)f(\alpha) \qquad \text{Eq. 1}$$

Where α is the fraction decomposed at time t, k(T) is the temperature dependent function and f(α) is the conversion function dependent on the mechanism of decomposition. It has been established that the temperature dependent function k(T) is of the Arrhenius type and can be considered as the rate constant k.

$$k = A\, e^{-E^*/RT} \qquad \text{Eq. 2}$$

Where R is the gas constant in ($Jmol^{-1}K^{-1}$). Substituting equation 2 into equation 1, gives;

$$d\alpha/dT = (A/\varphi\, e^{-E^*/RT})f(\alpha) \qquad \text{Eq. 3}$$

Where φ is the linear heating rate dT/dt. On integration and approximation, this equation can be obtained in the following form

$$\ln g(\alpha) = -E^*/RT + \ln[AR/\varphi E^*] \qquad \text{Eq. 4}$$

ISSN: 2319-8753

International Journal of Innovative Research in Science, Engineering and Technology

(An ISO 3297: 2007 Certified Organization)

Vol. 3, Issue 8, August 2014

Where g(α) is a function of α dependent on the mechanism of the reaction. Several techniques have been used for the evaluation of temperature integral. Most commonly used methods for this purpose are the differential method of Freeman and Carroll [17] integral method of Coat and Redfern [19], the approximation method of Horowitz and Metzger [22].

In the present investigation; the general thermal behaviors of the $2[La(NO_3)_3.MgCl_2.11Al(NO_3)_3.19C_4H_6O_6]$ in terms of stability ranges, peak temperatures and values of kinetic parameters, are shown in Fig.4 and Table 1. The kinetic parameters have been evaluated using the following methods and the results obtained by these methods are compared with one another. The following two methods are discussed in brief.

i- Coats- Redfern equation

The Coats-Redfern equation, which is a typical integral method, can be represented as:

$$\int_0^{\infty} d\alpha/(1-\alpha)^n = (A/\varphi) \int_{T1}^{T2} e^{-E^*/RT}\, dT \qquad \text{Eq. 5}$$

For convenience of integration the lower limit T_1 is usually taken as zero. This equation on integration gives;

$$\ln[-\ln(1-\alpha)/T^2] = -E^*/RT + \ln [AR/\varphi E^*] \qquad \text{Eq. 6}$$

A plot of left-hand side (LHS) against 1/T was drawn. E^* is the energy of activation in kJ mol^{-1} and calculated from the slop and A in (s^{-1}) from the intercept value. The entropy of activation ΔS^* in ($JK^{-1}mol^{-1}$) was calculated by using the equation:

$$\Delta S^* = R \ln(Ah/k_B T_s) \qquad \text{Eq. 7}$$

Wherek_B is the Boltzmann constant, h is the Plank's constant and $T_s$is the DTG peak temperature [23].

ii- Horowitz-Metzger equation:

The Horowitz-Metzger equation is an illustrative of the approximation methods. These authors derived the relation:

$$\log[\{1-(1-\alpha)^{1-n}\}/(1-n)] = E^*\theta/2.303RT_s^2 \quad \text{for } n\neq 1 \qquad \text{Eq. 8}$$

Where $\theta = T - T_s$, $w_\gamma = w_\alpha - w$, w_α = mass loss at the completion of the reaction; w = mass loss up to time t. The plot of $\log[\log(w_\alpha/ w_\gamma)]$ vsθ was drawn and found to be linear from the slope of which E^* was calculated. The pre-exponential factor, A, was calculated from the equation:

$$E^*/RT_s^2 = A/[\varphi \exp(-E^*/RT_s)] \qquad \text{Eq. 9}$$

The entropy of activation, ΔS^*, was calculated from equation 7. The enthalpy activation, ΔH^*, and Gibbs free energy, ΔG^*, were calculated from;

$$\Delta H^* = E^* - RT \qquad \text{Eq. 10}$$

$$\Delta G^* = \Delta H^* - T\Delta S^* \qquad \text{Eq. 11}$$

From the point of view of TG analysis, the most important and reliable kinetic parameter is the activation energy, which can be related with the thermal stability of the parent compound and in some cases, with some IR data. As can be verified by looking to Table 1 data, significantly, the $2[La(NO_3)_3.MgCl_2.11Al(NO_3)_3.19C_4H_6O_6]$ parent compound exhibits a positive ΔS for the thermal degradation process. This fact is probably related with the fact that this compound exhibits the higher ΔH value. It means; if it is the most difficult to remove ligands from this compound, the degree of disorder introduced into the system by such process could be positive. In this kind of process it is always necessary to

ISSN: 2319-8753

International Journal of Innovative Research in Science, Engineering and Technology

(An ISO 3297: 2007 Certified Organization)

Vol. 3, Issue 8, August 2014

take into account that under heating a solid (the compound) is producing a new solid (carbonates) and a gaseous product. Therefore, the ΔS value is for this "large system", and not only to the main decomposition process product. Hence, the overall ΔS value can be positive, as consequence of the entropy changes in the gaseous and solid products (in this last case, the formation of a new crystalline lattice). Since La(III), Mg(II) and Al(III) exhibit a closer shell, the higher E_a value to the $2[La(NO_3)_3.MgCl_2.11Al(NO_3)_3.19C_4H_6O_6]$ suggests that a small cation with covalent radius of an average 0.772 angstrom can stabilize (provide a most stable crystalline lattice) in a most effective way a compound with three metal ions.

Table 1: Kinetic parameters calculated using the Coats-Redfern (CR) and Horowitz-Metzger (HM).

Horowitz-Metzer					**Coats-Redfen**					
E/ kJmol^{-1}	Z/ s^{-1}	ΔS/ Jmol^{-1}K^{-1}	ΔH/ kJmol^{-1}	ΔG/ kJmol^{-1}	E/ kJmol^{-1}	Z/ s^{-1}	ΔS/ Jmol^{-1}K^{-1}	ΔH/ kJmol^{-1}	ΔG/ kJmol^{-1}	r
260	6.00E+22	202	261	146	239	8.00E+21	162	244	152	0.9691

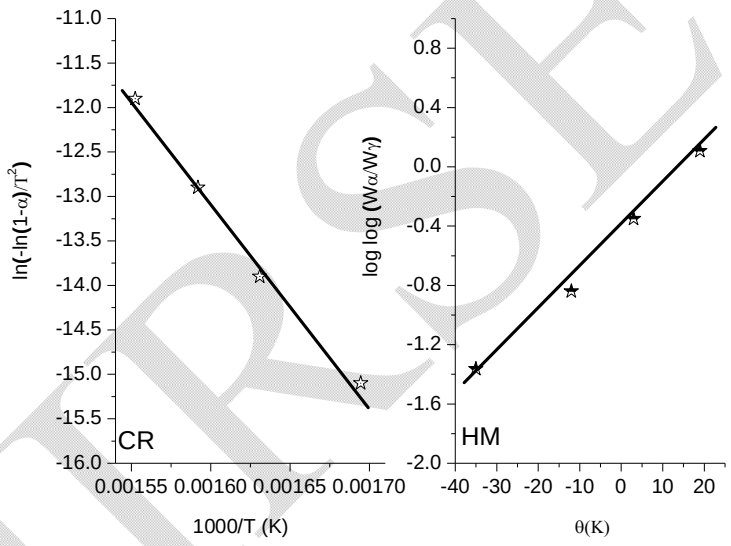

Fig.4: Horowitz-Metzger (HM) and Coats-Redfern (CR) plots for $[La(NO_3)_3.MgCl_2.11Al(NO_3)_3.19C_4H_6O_6]$ adduct.

3.4. XRD analysis

XRD was performed with several samples that had been exposed for various temperatures, as shown in Fig 5. The intensities of the peaks were varied; according to the calcination temperatures. At temperature of 1000 ^oC, there was not any sharp significant diffraction peaks detected, so that, there is no formation of any crystal phase, and all the materials are not well crystallized. When the calcination temperature was raised to 1100 ^oC, reflections associated with magentoplumbite phase appeared and were the only features in the XRD spectra. These diffraction peaks belong to a pure single phase of hexaaluminate $LaMgAl_{11}O_{19}$ (JCPDS 26-0873). The peaks were more intense at 1200 and 1300 ^oC, which clearly attributed to well-crystallized particles of $LaMgAl_{11}O_{19}$ compound [9-12].

ISSN: 2319-8753

International Journal of Innovative Research in Science, Engineering and Technology

(An ISO 3297: 2007 Certified Organization)

Vol. 3, Issue 8, August 2014

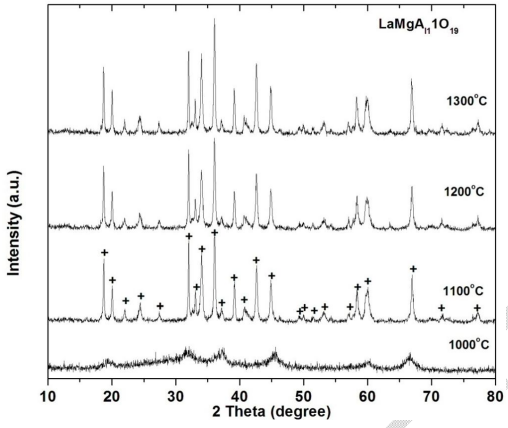

Fig. 5: XRD patterns of $LaMgAl_{11}O_{19}$ from lanthanum-magnesium - aluminum tartrate precursor treated at different temperatures (1000-1300°C) for 2 h.

3.5. SEM examinations

Images of the SEM examinations are shown in Fig. 6. It can be seen that the sample annealed at 1000 °C for 2 hr is composed of randomly irregular shape of $LaMgAl_{11}O_{19}$ powders. As the annealing temperature increased to 1100 °C, the crystal growth of the powder is clearly anisotropic. Moreover, the crystal morphology is large platelet –like grains, which is a characteristic of hexaaluminates. One possible explanation is that using the tartaric acid method exhibit fine and well-crystalline particles at this relatively low calcination temperature. Other important information is the x-ray maps for the elements of lanthanum, magnesium, aluminum and oxygen, as shown in Fig 7. Images in the Figure depict homogenous distribution of constituents of the sample annealed at 1100 °C. Usually EDS mapping is used in order to illustrate the distribution of different elements of the phase. Whereas, the EDS mapping is not related to the particle shape of the phase. In this case, the EDS were introduced for mapping, in order to prove the homogeneous distribution of the elements of hexaaluminate throughout the specimen.

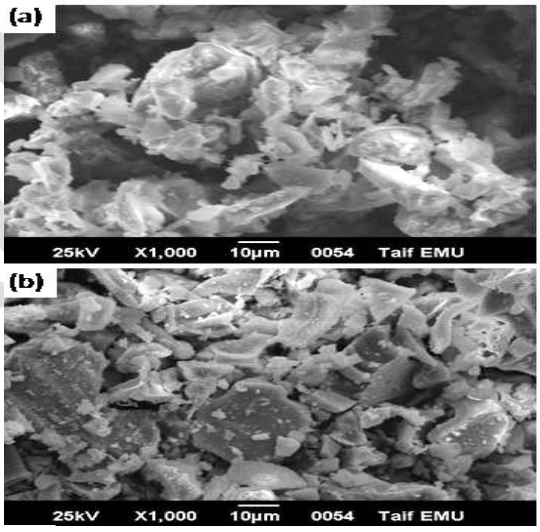

Fig. 6: Effect of annealing temperatures on the microstructure of synthesized $LaMgAl_{11}O_{19}$ powders obtained from tartrate precursors annealed for 2h. (a) 1000°C, (b) 1100°C

ISSN: 2319-8753

International Journal of Innovative Research in Science, Engineering and Technology

(An ISO 3297: 2007 Certified Organization)

Vol. 3, Issue 8, August 2014

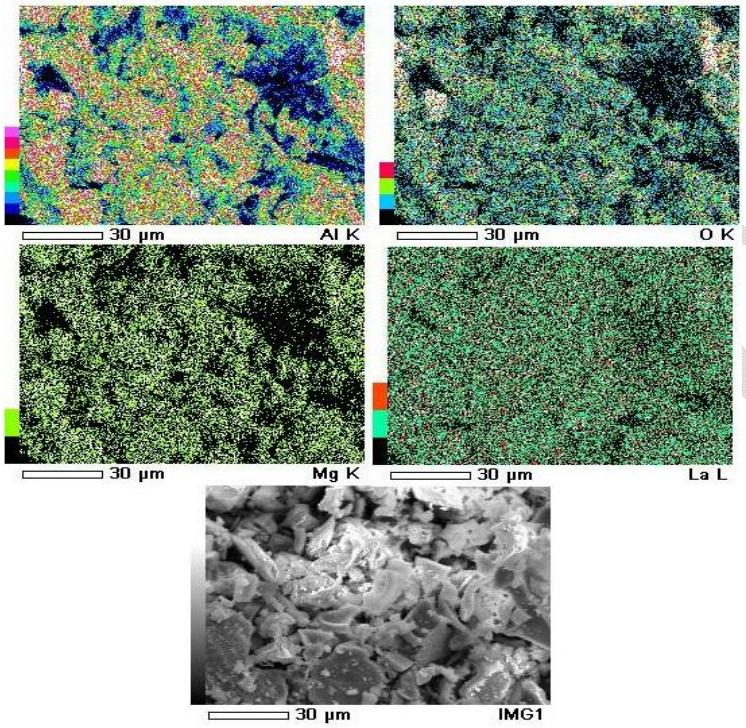

Fig. 7: Microstructure maps for constituent elements of synthesized $LaMgAl_{11}O_{19}$ powders obtained from tartrate precursors annealed at 1100 ^{o}C for 2h.

IV. CONCLUSIONS

Magnesium substituted lanthanum hexaaluminate ($LaMgAl_{11}O_{19}$) has been synthesized by a co-precipitation method, using tartaric acid as a precursor. The XRD patterns showed that almost all the prepared samples remained amorphous below and at 1000^{0}C. A pure single crystal phase of $LaMgAl_{11}O_{19}$ was formed at 1100^{0}C. The use of tartaric acid technique enhances the growth of fine and well-crystalline particles at relatively low calcination temperature. Therefore, the resultant microstructure of the $LaMgAl_{11}O_{19}$ powder could be a promising material for TBCs applications.

REFERENCES

1. Xiaolong Chen, Yanfei Zhang ,J. Eur. Ceram. Soc. 30 (2010) 1649-1657.
2. Fengxiang Yin , ShengfuJi ,Pingyi Wu, Fuzhen Zhao ,Chenngyue Li ,J.MolecularCatalsis A: Chemical 294 (2008) 27-36 .
3. Ren-Xian Zhu, Zhan-GuoLiu,Jia-Hu,Yu Zhou Ceramics International 39 (2013)8841-8846.
4. D.R. Clarke, C.G. Levi. Material design for the next generation of thermal barrier coating. Annu Rev Mater Res 33 (2003) 383.
5. A.G. Evans, D.R. Clarke, C.G. Levi, J. Eur. Ceram. Soc. 28 (2008) 1405.
6. Robert Vaben,Maria Ophelia Jarligo, Surf. Coat. Technol205 (2010) 938.
7. A. Azzopardi, R. Mevrel, B.S. Ramond, E. Olson, K. Stiller, Surf. Coat. Technol131 (2004) 177.
8. C. Friedrich, R. Gadow, T. Schirmer, J. Therm. Spray. Technol 10(4) (2001) 592.
9. R. Gadow, M. Lischka, Surf. Coat. Technol151 (2002) 392.
10. M.K. Cinibulk, J. Mater. Sci. Lett. 14 (1995) 651.
11. Z. Negahdari, M. Willert-Porada, F. Scherm, J. Eur. Ceram. Soc. 30 (2010) 3103.
12. Z. Negahdari, M. Willert-Porada, Adv. Eng. Mater. 11, 12 (2009) 1034
13. M. Kantcheva, J. Catal. 204 (2001) 479.
14. M. Kantcheva, M.U. Kucukkal, S. Suzer, J. Catal. 190 (2000)144.
15. Ozawa, M., Onoe, R. and Kato, H., J. Alloys Comp., 2006, 408–412, 556–559.

ISSN: 2319-8753

International Journal of Innovative Research in Science, Engineering and Technology

(An ISO 3297: 2007 Certified Organization)

Vol. 3, Issue 8, August 2014

16. Dean, John A., Lange's Handbook of Chemistry (12th ed.). McGraw-Hill,1979, pp. 3–120.
17. E.S. Freeman, B. Carroll, J. Phys. Chem., 62 (1958) 394
18. J. Sestak, V. Satava, W.W. Wendlandt, Thermochim. Acta, 7 (1973) 333
19. A.W. Coats, J.P. Redfern, Nature, 201 (1964) 68.
20. T. Ozawa, Bull. Chem. Sot. Jpn.,38 (1965) 1881.
21. W.W. Wendlandt, Thermal Methods of Analysis, Wiley, New York, 1974.
22. H.W. Horowitz, G. Metzger, Anal. Chem., 35 (1963) 1464.
23. Brand, P., Troschke, R. and Weigelt, H., Cryst.Res. Technol., 2006, 24(7), 671–675.